Insights into the Catalytic Mechanism of HlyC, the Internal Protein Acyltransferase That Activates *Escherichia coli* Hemolysin Toxin†

Lesa M. S. Worsham, M. Stephen Trent,‡ Laurie Earls, Carrie Jolly, and M. Lou Ernst-Fonberg*

Department of Biochemistry and Molecular Biology, James H. Quillen College of Medicine, Box 70 581, East Tennessee State University, Johnson City, Tennessee 37614

Received May 21, 2001; Revised Manuscript Received August 15, 2001

ABSTRACT: Hemolysin, a toxic protein secreted by pathogenic *Escherichia coli*, is converted from nontoxic prohemolysin, proHlyA, to toxic hemolysin, HlyA, by an internal protein acyltransferase, HlyC. Acyl-acyl carrier protein (ACP) is the essential acyl donor. The acyltransferase reaction proceeds through two partial reactions and entails formation of a reactive acyl-HlyC intermediate [Trent, M. S., Worsham, L. M., and Ernst-Fonberg, M. L. (1999) *Biochemistry 38*, 9541−9548]. The ping pong kinetic mechanism implied by these findings was validated using two different acyl-ACP substrates, thus verifying the independence of the previously demonstrated two partial reactions. Assessments of the stability of the acyl-HlyC intermediate revealed an increased stability at pH 8.6 compared to more acidic pHs. Mutations of a single conserved histidine residue essential for catalysis gave minimal activity when substituted with a tyrosine residue and no activity with a lysine residue. Unlike numerous other His23 mutants, however, the H23K enzyme showed significant acyl-HlyC formation although it was unable to transfer the acyl group from the proposed amide bond intermediate to proHlyA. These findings are compatible with transient formation of acyl-His23 during the course of HlyC catalysis. The effects of several other single site-directed mutations of conserved residues of HlyC on different portions of the reaction progress were examined using a 39 500 kDa fragment of proHlyA which was a more effective substrate than intact proHlyA.

Fatty acylation of internal residues of a protein is a means of modifying its biological behavior. While numerous instances of protein internal fatty acylation, generally via thiol esterification of cysteine residues, have been reported, the acyltransferases catalyzing these reactions have been elusive. Although there are several reports of posttranslational modification by internal fatty acylation of specific proteins through amide linkage (*1*−*4*), the enzymes have been neither isolated nor characterized. The extent of internal fatty acylation via amide linkage of mammalian proteins is unknown. However, acylation of cellular protein with endogenously synthesized fatty acids in a mouse muscle cell line indicated that at least 30% of protein-bound palmitate was present in amide linkage with undefined residues (*5*).

The toxicity of hemolysin (HlyA),[1] a protein toxin secreted by pathogenic *Escherichia coli*, rests upon the acylation of two specific internal lysine residue ϵ-amino groups. It is one of the RTX (repeats in toxin) family of homologous, membrane-active toxins of similar mechanism produced by different Gram-negative bacteria (*6*, *7*). Nontoxic protoxin (proHlyA) is posttranslationally converted intracellularly to HlyA, a cytolytic toxin, by the action of a cosynthesized protein, HlyC, an internal protein acyltransferase (*8*). Acyl-ACP is the obligate acyl donor (*9*, *10*).

Recently, we reported the separate subcloning and expression of each of the proteins participating in the internal acylation of proHlyA to form HlyA and characterized the acyltransferase, HlyC, and the reaction it catalyzes (*10*). Notably, a reactive acyl-HlyC intermediate is formed, and the acyltransferase reaction consists of two partial reactions (*11*):

$$\text{acyl-ACP} + \text{HlyC} \leftrightarrow [\text{HlyC}\cdot\text{acyl-ACP}] \leftrightarrow \text{acyl-HlyC} + \text{ACPSH}$$

$$\text{acyl-HlyC} + \text{proHlyA} \leftrightarrow [\text{proHlyA}\cdot\text{acyl-HlyC}] \leftrightarrow \text{HlyA} + \text{HlyC}$$

$$\text{sum: acyl-ACP} + \text{proHlyA} \leftrightarrow \text{HlyA} + \text{ACPSH}$$

Comparison of deduced amino acid sequences of 13 RTX C proteins reveals extensive homology (*12*); 21% of the 170

† This work was supported by National Institutes of Health Grants R01-GM62121 and R15-GMOD54337 and by a grant from the American Heart Association, Southeast Affiliate.

* To whom correspondence should be addressed at the Department of Biochemistry and Molecular Biology, James H. Quillen College of Medicine, Box 70 581, East Tennessee State University, Johnson City, TN 37614. Phone: (423) 439-4656. Fax: (423) 439-8235. E-mail: ernstfon@etsu.edu.

‡ Present address: Department of Biochemistry, Box 3711, Duke University Medical Center, Durham, NC 27710.

[1] Abbreviations: proHlyA, hemolysin A protoxin; HlyA, hemolysin A toxin; RTX, repeats in toxin; HlyC, acyl-ACP-proHlyA acyltransferase; ACP, acyl carrier protein; ACPSH, acyl carrier protein with a free prosthetic group thiol; lauroyl-ACP, acyl carrier protein with a 12 carbon acyl chain covalently attached to the prosthetic group thiol; myristoyl-ACP, acyl carrier protein with a 14 carbon acyl chain covalently attached to the prosthetic group thiol; acyl-ACP, acyl carrier protein with a long-chain fatty acyl covalently attached to the prosthetic group thiol; Hepes, *N*-(2-hydroxyethyl)piperazine-*N*′-2-ethanesulfonic acid; EDTA, ethylenediaminetetraacetic acid; SDS, sodium dodecyl sulfate; PAGE, polyacrylamide gel electrophoresis; PCR, polymerase chain reaction; DFP, phosphorofluoridic acid bis(1-methylethyl)ester.

10.1021/bi011032h CCC: $20.00
Published on Web 10/20/2001

Table 1: Primers Used To Construct ProHlyA Fragment A and HlyC Mutants

name[a]	sequence (5′ to 3′)
fragment A 5′	CTCAGTCCTCATTACCCAGCAACATTG
fragment A 3′	CTAATCACCGCCATAGAGCTGGTCATCTC
S19AS20A 5′	GTATCCTGGCTATGGGCCGCTGCTCCACTACACAGAAACTGG
S19AS20A 3′	CCAGTTTCTGTGTAGTGGAGCAGCGGCCCATAGCCAGGATAC
S20C 5′	CCTGGCTATGGGCCAGTTGTCCACTACACAGAAACTGG
S20C 3′	CCAGTTTCTGTGTAGTGGACAACTGGCCCATAGCCAGG
S20H 5′	CCTGGCTATGGGCCAGTCATCCACTACACAGAAACTGG
S20H 3′	CCAGTTTCTGTGTAGTGGATGACTGGCCCATAGCCAGG
S20T 5′	CCTGGCTATGGGCCAGTACTCCACTACACAGAAACTGG
S20T 3′	CCAGTTTCTGTGTAGTGGAGTACTGGCCCATAGCCAGG
H23D 5′	GGCTATGGGCCAGTTCTCCACTAGACAGAAACTGGCCAGTATC
H23D 3′	GATACTGGCCAGTTTCTGTCTAGTGGAGAACTGGCCCATAGCC
H23K 5′	GGGCCAGTTCTCCACTAAAAAGAAACTGGCCAGTATC
H23K 3′	GATACTGGCCAGTTTCTTTTTAGTGGAGAACTGGCCC
H23Y 5′	GGCTATGGGCCAGTTCTCCACTATACAGAAACTGGCCAGTATC
H23Y 3′	GATACTGGCCAGTTTCTGTATAGTGGAGAACTGGCCCATAGCC
Q43A 5′	CCCGCAATACAGGCTAACGCTTATGTTTTATTAACCCGGG
Q43A 3′	CCCGGGTTAATAAAACATAAGCGTTAGCCTGTATTGCGGG

[a] Letters are one-letter amino acid abbreviations. The template for proHlyA fragment A was pTXA1; that for the HlyC mutations was pTXC2.

residues in HlyC are identical among the RTX C proteins. The site of acylation during the transient formation of acyl-enzyme intermediate is likely a conserved residue. Chemical modification experiments and site-directed mutation analysis of conserved residues capable of bearing acyl groups have shown His23 to be essential for activity and certain conserved tyrosine and serine residues to be important in HlyC catalysis (*11*, *13*, *14*). The crucial roles of His23 and Ser20 and the nature of the acyl-HlyC intermediate have been further examined. The kinetic mechanism implied by the demonstration of the substituted enzyme and the partial reactions has been established using acyl-ACPs bearing two different acyl groups. In conjunction with these experiments that have served to clarify the reaction mechanism, a more stable protein to explore the nature of internal protein acylation, a fragment of proHlyA, was developed.

EXPERIMENTAL PROCEDURES

Materials. [1-^{14}C]Myristate and [1, 3-^{3}H]DFP were from New England Nuclear; [1-^{14}C]laurate was from Amersham Life Science. *Eco*RV, *Dpn*-I, and Deep Vent DNA polymerase were from New England Biolabs. *Pfu Turbo* DNA polymerase was from Stratagene. 3-(1-Pyridinio)-1-propanesulfonate was from Fluka. All chemicals were reagent grade. Urea-containing buffers were freshly prepared. Ni−NTA agarose was from Qiagen. Novagen was the source of alkaline phosphatase conjugated S-peptide and pET plasmids.

Bacterial Strains and Growth Media and DNA. E. coli strains were BL21(DE3)pLysS from Novagen and XL-2 Blue from Stratagene. Cells were grown in Luria broth except for expression of HlyC and its mutants; these were grown in minimal media, induced with 1 mM isopropyl β-D-thiogalactopyranoside at $A_{600nm} = 0.6$, and harvested after 3 h. Oligonucleotides used for subcloning the fragment of the *hlyA* gene or site-directed mutagenesis of *hlyC* were from Integrated DNA Technologies and are given in Table 1. DNA between base pairs 2733 and 3638 of the pHly152 *hly* determinant (*15*) encoding a portion of the *hlyA* gene designated fragment A was subcloned from pTXA1 (*10*) using PCR with Deep Vent DNA polymerase. The purified amplified DNA was blunt end ligated into the *Eco*RV site of pET-30(b) which encoded an N-terminal His_6-S-tag fused with the fragment of proHlyA, resulting in pTXAt1 which was transformed into BL21(DE3)pLysS for expression.

Site-Directed Mutagenesis. Site-directed mutations in *hlyC* were generated by the round-circle PCR method described in the QuikChange Site-Directed Mutagenesis Kit protocol (Stratagene) using the plasmid pTXC2 as the reaction template (*13*). The rationale involved whole-plasmid PCR amplification using the mutagenic oligonucleotides shown in Table 1, one 5′ and one 3′ primer for each mutation. Residual native plasmid was digested with the *dam* methylation-specific restriction endonuclease, *Dpn*-I, and the PCR product containing the mutation was transformed into XL2-Blue cells for efficient cloning of nonmethylated DNA. Mutation of DNA was confirmed by DNA sequence analysis (*16*) at the Molecular Genetics Facility at the University of Georgia. Plasmids containing mutant HlyC inserts were designated pTXC2 along with a description of the mutation, and the vectors containing mutant HlyCs were transformed into BL21(DE3)pLysS for expression.

Proteins. Proteins were handled at 4 °C unless noted otherwise. ProHlyA, ACPSH, [^{14}C]lauroyl-ACP, and [^{14}C]myristoyl-ACP were obtained as described by Trent and colleagues (*10*). Lauroyl-ACP and myristoyl-ACP were purified and evaluated as described (*17*) and stored in aliquots at −80 °C.

HlyC expressed as a His_6-S-tag fusion protein from pTXC2 described previously (*13*) was employed for kinetics. Inclusion bodies from pTXC2 cells or its mutants were isolated from the cell lysate pellet (250 mL culture) and washed twice with 25 mM Hepes (pH 8), 5 mM EDTA, 1 mM dithiothreitol, 1% Triton X-100. Protein was solubilized from inclusion bodies with 5 mL of 25 mM Hepes (pH 8), 5 mM EDTA, 1 mM dithiothreitol, 6 M guanidine hydrochloride. Protein from inclusion bodies obtained from pTXC2 cells or mutants thereof was routinely refolded in the presence of mild solubilizing agents, nondetergent sulfobetaines, 3-(1-pyridinio)-1-propanesulfonate in this instance, as described by Vuillard and colleagues (*18*). The solution was clarified by centrifugation at 30000*g* for 30 min. Fusion protein was precipitated overnight at 65% $(NH_4)_2SO_4$ saturation, collected by centrifugation at 30000*g* for 30 min, and dissolved in 25

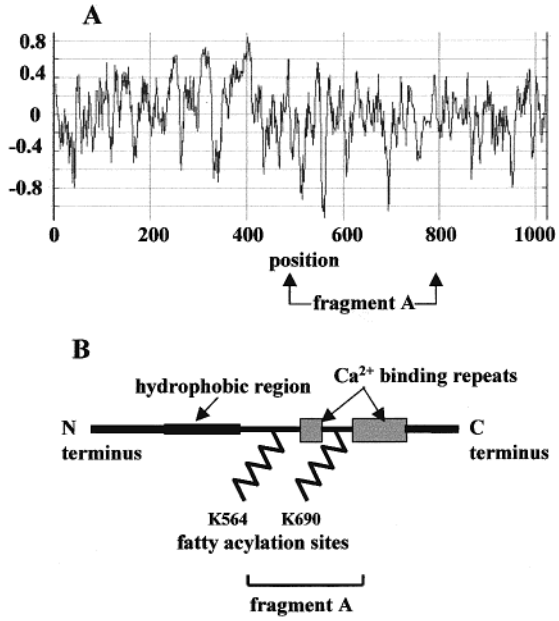

FIGURE 1: Hydrophobicity profile and structural schematic of proHlyA. Panel A shows the hydrophobicity profile of proHlyA and the portion of it that formed fragment A. Panel B is a schematic representation of the structural regions of proHlyA, and the approximate region forming fragment A is between brackets.

mM Hepes (pH 8), 5 mM EDTA, 1 mM dithiothreitol. It was stored in aliquots at −80 °C. Protein yield was ∼5 mg. Alternatively, urea extracts of inclusion bodies containing wild-type or mutant His_6-S-tag-HlyC were subjected to quick refolding to detect possible structural roles of mutant residues. Mutant and wild-type cultures of 5 mL were grown simultaneously, induced, harvested, and stored at −20 °C. At the time of use, cells were thawed, disrupted, and analyzed for HlyC activity as previously described (*13*).

N-terminal His_6-S-tag fusion fragment A was hyperexpressed from cells grown as described previously for pTXA1 expression (*10*). Following induction and harvest of a 250 mL culture and storage of the cell pellet at −20 °C, fragment A was isolated from inclusion bodies. After brief exposure of the thawed cells to ultrasound, the mixture was diluted with 200 mL of 25 mM Hepes (pH 8), 5 mM EDTA, 1 mM dithiothreitol, collected by centrifugation at 20000*g* for 20 min, washed with 220 mL of the same buffer, and collected as before. The pellet was suspended with occasional gentle agitation in 1 mL of the same buffer containing 6 M urea for 1.5 h; then the supernatant solution was collected by centrifugation and stored in aliquots at −80 °C. The protein yield was 6.5 mg of which 92% was fragment A. The 39 500 kDa protein included amino acid residues 472−780 of the 1024 residues constituting proHlyA. The relatively hydrophobic portion of proHlyA near the N terminus (Figure 1) and several of the Ca^{2+} binding repeats were eliminated in fragment A. ProHlyA has two fatty acylation sites, the ϵ-amino groups of lysine residues 564 and 690, and both sites were preserved, Lys140 and Lys 266, in fragment A. Fragment A of greater purity was obtained by washing inclusion bodies from 250 mL of cells in 25 mM Hepes (pH 8), 0.5 M NaCl, 5 mM imidazole and bringing the inclusion bodies up in 5 mL of 25 mM Hepes (pH 8), 0.5 M NaCl, 5 mM imidazole, 6 M urea. After 1.5 h with occasional gentle agitation, the urea solution was clarified by centrifugation, mixed with 2 mL of Ni−NTA agarose, and gently agitated overnight. The agarose was rinsed into a column using the urea buffer and washed with 25 mL more of the urea buffer. The column was washed with 20 mL of buffer that contained 20 mM imidazole, and fragment A was eluted from the column by washing with 6 mL of buffer that contained 500 mM imidazole. The solution was divided into two halves; each was concentrated in a 10 000 cutoff Centricon (Amicon). One was washed with 2 mL of 25 mM Hepes (pH 8), 5 mM EDTA, 1 mM dithiothreitol and brought up in the same buffer; the other was also washed and then brought up in the same buffer which contained 6 M urea.

Treatment of HlyC with DFP. HlyC wild-type and mutant S20A, each at 1.1 μM, were treated with 12 μM [1,3-^{3}H]-DFP, 8.4 Ci/mmole in the presence and absence of 2.3 μM myristoyl-ACP in 100 mM Hepes (pH 7.5) (*19*). The reaction volume was 100 μL. After 1 h at 25 °C, reactions were made 10% in trichloroacetic acid and kept on ice for 45 min and then centrifuged at 13600*g* for 5 min. The protein pellet was washed with 500 μL of cold acetone. Precipitated protein was dissolved in 20 μL of 8 M urea + 20 μL of 2% SDS sample buffer and subjected to SDS−15%PAGE followed by fluorography as described below.

Protein Determination. Protein was measured as described by Bradford (*20*).

Chemical Cross-Linking of Proteins Involved in Fragment A Acylation. Reactions were set up as described previously for assay of HlyC activity (*10*), and protein contents were those given in the Figure 2 legend. Reactions were exposed to 10 mM dimethyl suberimidate for 10 min at 25 °C. Reactions were halted by the addition of 1 M ammonium acetate to a final concentration of 100 mM, and proteins were precipitated at 4 °C with 10% trichloroacetic acid. After 45 min, precipitated protein was collected by centrifugation at 13600*g* for 5 min and washed with 500 μL of acetone; the pellet was collected again by centrifugation. Protein was dissolved in 20 μL of 8 M urea and 20 μL of 2% SDS sample buffer and analyzed as described in the Figure 2 legend.

Measurement of Acyl-HlyC Stability. [^{14}C]Myristoyl-HlyC was generated by incubating 18 μM HlyC + 4 μM [^{14}C]myristoyl-ACP in 100 μL of 50 mM Hepes (pH 8) for 5 min at 25 °C. Reactions were brought to 60% saturation with 100% saturated neutral ammonium sulfate, kept on ice for 45 min, and then centrifuged at 13600*g* for 5 min. Myristoyl-ACP did not precipitate under these conditions; thus, precipitates consisted of HlyC and [^{14}C]myristoyl-HlyC. Each precipitate was dissolved in one of the following solutions and kept at 25 °C for 30 min: 250 mM acetate (pH 5); 250 mM Hepes (pH 6.5); 250 mM Hepes (pH 6.5), 500 mM dithiothreitol; 250 mM Hepes (pH 6.5), 1 M hydroxylamine; 100 mM Hepes (pH 8); 250 mM Hepes (pH 8.6); 250 mM Hepes (pH 8.6), 500 mM dithiothreitol; 250 mM Hepes (pH 8.6), 1 M hydroxylamine. At least three samples were examined independently for each condition. Two approaches were used to measure acyl-HlyC after its formation and exposure to various conditions. First, [^{14}C]myristoyl-HlyC was isolated by ammonium sulfate precipitation at neutrality, washed free of residual [^{14}C]myristoyl-ACP, ACPSH, and [^{14}C]myristate with 50% 2-propanol, and measured using the acyl transfer assay procedure of Trent and colleagues (*10*). Second, acyl-HlyC stability upon exposure to diverse conditions was documented by separation of

the reaction components by SDS−15%PAGE, fluorography, and scanning in the way described below.

Gel Electrophoresis, Fluorography, and Western Blotting. The purity of each protein used was assessed by densitometry following SDS−PAGE according to Laemmli (*21*). Fluorograms and gels were scanned using a Hewlet-Packard ScanJet 5200C; the scan densities were analyzed with Un-Scan-It software by Silk Scientific. HlyC mutants and wild-type were ~85% pure, proHlyA was ~90% pure, and unpurified fragment A was ~92% pure. Western blotting onto PVDF membrane (Bio-Rad) was done using a Bio-Rad Semi-Dry Electrophoretic transfer cell according to the manufacturers' instructions. Fluorography was done as previously described (*17*) using Enhance or Entensify (New England Nuclear) and Kodak BioMax MR film.

Measurement of Enzyme Activity. The rate of HlyC-catalyzed acyl transfer from [^{14}C]myristoyl-ACP or [^{14}C]lauroyl-ACP to proHlyA was measured as previously described (*10*). Previously unthawed aliquots of proHlyA and HlyC were used for each measurement. Reactions were initiated by the addition of acyl-ACP. Initial velocity kinetic data were analyzed by fitting eq 1 directly in the hyperbolic form with an unweighted analysis as described by Wilkinson (*22*) using Hyper (Emmet-Drury Software) where V_{max} is the maximal velocity and K_m is the Michaelis constant for the varied substrate S.

$$V = \frac{V_{max}[S]}{[S] + K_m} \quad (1)$$

These analyses yielded the kinetic parameters reported. Data were also examined using several linear forms using a computer program previously described (*23*). Agreement among all methods was required for acceptance of data. Steady-state enzyme kinetics were done to distinguish between the two basic mechanisms described in rate equations 2, a ping pong mechanism, and 3, a sequential mechanism.

$$v = \frac{V_{max}[A][B]}{K_m^{B}[A] + K_m^{A}[B] + [A][B]} \quad (2)$$

$$v = \frac{V_{max}[A][B]}{K_m^{B}[A] + K_m^{A}[B] + [A][B] + K_S^{A}K_m^{B}} \quad (3)$$

K_m^{A} and K_m^{B} are the Michaelis constants for substrates A and B. Initial velocity patterns shown were obtained by measuring acyl transfer as a function of proHlyA at different fixed concentrations of acyl-ACP.

RESULTS

Preparation and Characteristics of ProHlyA Fragment. The 39 500 kDa fragment including amino acid residues Ser472 through Asp780 of proHlyA, fragment A, which contained both proHlyA acylation sites, was hyperexpressed and purified (Figure 2A). It functioned as a substrate for the internal acyltransferase HlyC. Using the routine assay previously described (*10*) where all other factors were invariant and either proHlyA or fragment A was at 1 μM, the following amounts of acyl transfer were measured. With

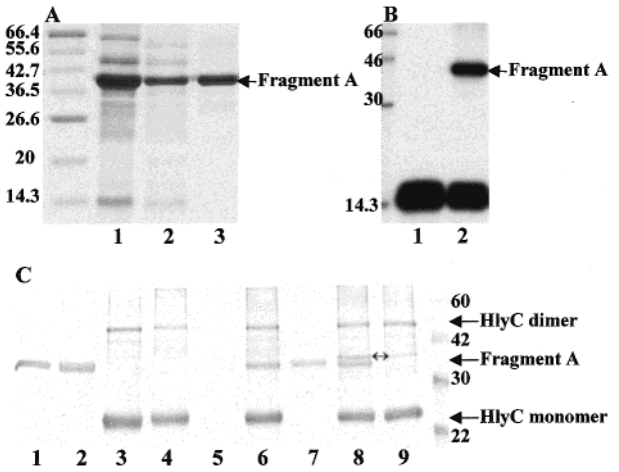

FIGURE 2: SDS−PAGE and Western blot analyses of fragment A purification and reactivity. Molecular size standards shown in panels A−C are in kDa. Panel A is a Coomassie-stained SDS−15% PAGE showing fragment A purification progress. Proteins from the following sources were applied: lane 1, 15 μg of inclusion body protein; lane 2, 5 μg of protein, buffered urea extract of inclusion bodies; lane 3, 5 μg of protein, 20 mM buffered imidazole Ni−NTA agarose eluate. Panel B is a fluorogram of reactants exposed to dimethyl suberimidate followed by separation on SDS−15% PAGE showing radioactive acyl group transfer from myristoyl-ACP to fragment A. Reactions of 100 μL prepared at pH 8 contained 2 μM [^{14}C]myritstoyl-ACP plus the following proteins: lane 1, 2 μM HlyC; lane 2, 2 μM HlyC + 1 μM fragment A. Panel C depicts interactions between different reactants in the presence and absence of dimethyl suberimidate separated by SDS−15% PAGE and then Western-blotted and probed with alkaline phosphatase-conjugated S-peptide. HlyC and fragment A contained N-terminal S-tags. Assay reactions of 100 μL were prepared, treated with dimethyl suberimidate unless noted otherwise, and processed as described under Experimental Procedures. The reactions contained the following substances: lane 1, 1 μM fragment A with no dimethyl suberimidate; lane 2, 1 μM fragment A; lane 3, 2 μM HlyC with no dimethyl suberimidate; lane 4, 2 μM HlyC; lane 5, 2 μM myristoyl-ACP; lane 6, 1 μM fragment A + 2 μM HlyC; lane 7, 1 μM fragment A + 2 μM myristoyl-ACP; lane 8, 1 μM fragment A + 2 μM myristoyl-ACP + 2 μM HlyC; lane 9, 2 μM myristoyl-ACP + 2 μM HlyC. The double-headed arrow between lanes 8 and 9 shows a band in each lane formed by the heterodimer of HlyC and myristoyl-ACP.

intact proHlyA at 1 μM, 32.5 ± 3 pmol of myristate was transferred/assay; a comparable preparation of fragment A at 1 μM, shown in Figure 2A, lane 2, transferred 59.7 ± 6 pmol/assay. Further purification on a nickel-charged resin of fragment A which bore an N-terminal His tag resulted in a purified protein (Figure 2A, lane 3) which had an activity at 1 μM of 55.3 ± 8 pmol/assay. Fragment A, in contrast to intact proHlyA, tolerated purification and freezing and thawing with no loss of activity; upon removal of urea from its storage buffer, however, its substrate efficacy was reduced to 22.1 ± 0.1 pmol of acyl group transferred/assay at 1 μM fragment A. Acylation of fragment A is shown in Figure 2B, a fluorogram in which the radiolabeled myristoyl group was detected as it migrated from myristoyl-ACP (lanes 1 and 2 lower bands) to fragment A, forming radiolabeled fragment A, the band at ~40 kDa in lane 2.

The proHlyA acylation reaction proceeds in two partial reactions via a substituted enzyme acyl-HlyC formed from partial reaction 1 between acyl-ACP and HlyC; there is no ternary complex formation (*10*, *11*). Fragment A acylation apparently proceeded similarly as shown in the blot in Figure

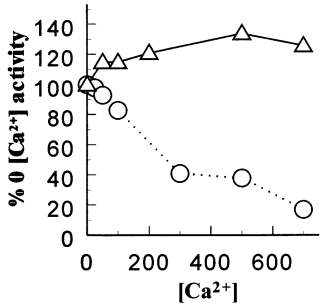

FIGURE 3: Effects of Ca^{2+} concentration on proHlyA and fragment A as substrates for internal acylation. Acyl transfer catalyzed by HlyC was measured as previously described (*10*); proHlyA and fragment A assay concentrations were 2 μM. Ca^{2+} concentration is in micromoles. Fragment A data are shown as (△) connected by a solid line; proHlyA data are represented by (○) connected by a dotted line.

2C where S-tag labels attached to HlyC and fragment A were detected after dimethyl suberimidate cross-linking of various combinations of enzyme and substrates. Lanes 1 through 4 show fragment A and HlyC each alone and each cross-linked alone; no novel bands were generated by dimethyl suberimidate treatment. Lane 5 shows, as expected, nothing from unlabeled myristoyl-ACP. Lanes 6 and 7 analyzed dimethyl suberimidate treatment of fragment A with HlyC and myristoyl-ACP, respectively, and no new bands were detected. Lane 8 cross-linking mix contained HlyC with fragment A and myristoyl-ACP, and a new, discrete band was generated immediately above the fragment A band. An identically sized new band was generated when the cross-linking reaction contained only HlyC and myristoyl-ACP (lane 9); this band and its counterpart in lane 8 are formed by the heterodimer of HlyC and myristoyl-ACP demonstrated previously (*10*, *11*). Furthermore, the same new band was discerned with chicken anti-ACP antibodies visualized with phosphorylase-conjugated anti-chicken immunoglobulin (not shown). No ternary complex (~71 kDa) formation among myristoyl-ACP, HlyC, and fragment A was detected with either probe.

ProHlyA conversion to HlyA is adversely affected by the presence of Ca^{2+} (*24*, *25*). Construction of fragment A resulted in removal of the portion of proHlyA beyond amino acid residue 800 that engages in exchangeable Ca^{2+} binding (Figure 1) (*26*−*28*). Examination of the effects of the presence of Ca^{2+} upon the acylation of proHlyA and fragment A by HlyC (Figure 3) showed that fragment A acylation was not impaired by Ca^{2+}. In contrast, proHlyA was increasingly refractory to acylation as the concentration of Ca^{2+} increased. Thus, the Ca^{2+} effect in the acyl transfer reaction was specific for proHlyA; the functions of enzyme, myristoyl-ACP, and fragment A were unaffected.

Characteristics of the Acyl-Enzyme Reaction Intermediate. Formation of a dynamic acyl-HlyC reaction intermediate enroute to the acylation of proHlyA is well documented (*10*, *11*). Observations of the chemical stability of myristoyl-HlyC under different conditions may provide clues to the nature of the chemical group acylated, and acyl-HlyC stability under various conditions was measured.

The acylation of HlyC was measured directly by reacting HlyC with [^{14}C]myristoyl-ACP, and following removal of unreacted myristoyl-ACP, the HlyC/myristoyl-HlyC mixture was exposed to varying conditions of pH and/or nucleophile

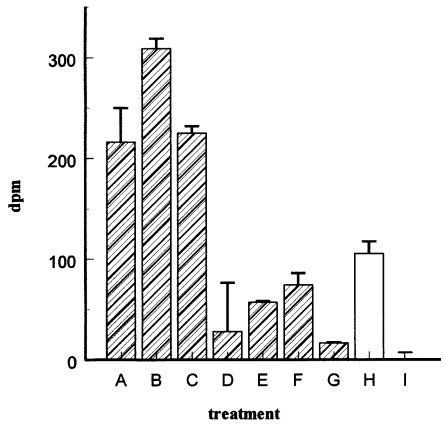

FIGURE 4: Myristoyl-HlyC stability under different conditions. [^{14}C]Acyl-HlyC formed under fixed conditions described under Experimental Procedures was subjected to different treatments and then measured by the assay described under Experimental Procedures. The hatched bars represent the following conditions to which acyl-HlyC generated from wild-type was exposed: A, pH 6.5; B, pH 8.6; C, 0.5 M dithiothreitol at pH 6.5; D, 0.5 M dithiothreitol at pH 8.6; E, 0.5 M imidazole at pH 8.6; F, 1 M hydroxylamine at pH 6.5; G, 1 M hydroxylamine at pH 8.6. Empty bars are conditions to which HlyC mutant C57A myristoyl-enzyme was exposed: H, 1 M hydroxylamine at pH 6.5; I, 1 M hydroxylamine at pH 8.6.

for 30 min. The reaction was then processed according to the assay procedure previously described (*10*) to remove residual myristoyl-ACP and free fatty acid, after which the remaining protein-bound radioactivity, myristoyl-HlyC, was measured (Figure 4). The acyl-enzyme intermediate was more stable at pH 8.6 compared to pH 6.5 (Figure 4, column B compared to column A). The presence of dithiothreitol at pH 6.5 slightly enhanced stability, but dithiothreitol at pH 8.6 led to a large disappearance of myristoyl-HlyC (Figure 4, column C compared to column D). The presence of a different nucleophile, imidazole, at basic pH also led to decreased stability (Figure 4, column E). Hydroxylamine catalyzed the hydrolysis of myristoyl-HlyC at pH 6.5 and 8.6; the effect was greater at pH 8.6 (Figure 4, columns F and G). HlyC contains a single cysteine residue, Cys57, conserved among all RTX C proteins, which had previously been considered as a candidate for acylation in the acyl transfer reaction. Sulfhydryl-reactive reagents and site-directed mutation analysis, however, showed that Cys57 has no evident function in enzyme activity; C57A possesses wild-type activity (*11*, *13*). While wild-type HlyC was theoretically capable of forming a thiol ester, C57A could not, and given the response of wild-type to hydroxylamine, the response to hydroxylamine of a mutant lacking any capacity to form a thiol ester was examined. For this purpose, the stability of myristoyl-C57A, a mutant devoid of SH groups, was measured. C57A acyl-enzyme intermediate exhibited sensitivity to hydroxylamine treatment at pHs 6.5 and 8.6, like that of wild-type (Figure 4, columns H and I compared to F and G).

In summary, the acyl-enzyme intermediate was less stable in a mildly acidic milieu compared to a basic environment, suggesting an amide rather than an ester bond. Further verification that the intermediate was not a thiol ester was the observation that mutant C57A acyl-enzyme intermediate which contained no cysteine residues responded like wild-type. Acyl-HlyC was subject to nucleophilic attack.

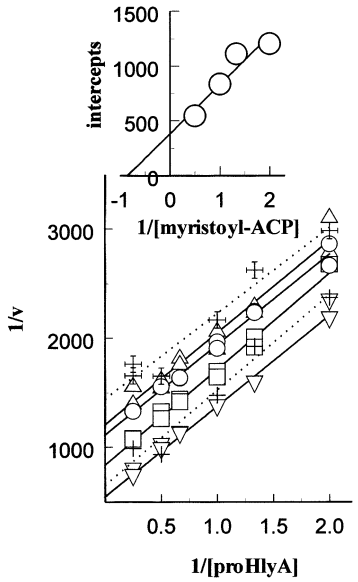

FIGURE 5: Steady-state kinetics of the HlyC-catalyzed reaction varying [proHlyA] at different fixed concentrations of myristoyl-ACP or lauroyl-ACP. The double-reciprocal primary plot shows initial velocity data for proHlyA obtained at the following fixed concentrations of myristoyl-ACP (solid lines): (△) 0.5 μM; (○) 0.75 μM; (□) 1 μM; (▽) 2 μM. Initial velocity data for proHlyA at the following fixed concentration of lauroyl-ACP (dotted lines) are also shown: (crosses) 0.5 μM; (plus signs) 1 μM. Velocities (v) are in arbitrary units. The inset shows the linear secondary plot of the respective double-reciprocal plot intercepts at different reciprocal concentrations (μM) of myristoyl-ACP. The assay procedure and methods of data analysis are given under Experimental Procedures.

Kinetic Mechanism of the Acyl Transfer Reaction. As mentioned above, internal acylation of proHlyA entails two partial reactions, a finding indicative of substituted enzyme formation, which has been previously shown (*10*, *11*). We have explored the relationship between acyl-HlyC formation and HlyC catalysis using site-directed mutation analysis (*11*, *13*, *14*). Furthermore, stability studies of the intermediate myristoyl-HlyC are reported above. These findings all imply a ping pong kinetic mechanism, but it is important to determine experimentally the steady-state kinetic mechanism of the HlyC-catalyzed reaction. Initial reaction velocities at varying proHlyA concentrations were measured at different fixed myristoyl-ACP concentrations, and the data plotted as double-reciprocal plots (Figure 5, solid lines) gave a set of parallel lines supporting a ping pong kinetic mechanism. An identical pattern of plots resulted when initial reaction rates were measured by varying myristoyl-ACP concentrations at different fixed proHlyA concentrations (data not shown). The kinetic constants of the reaction where both substrates are present in saturating amounts were determined from secondary plots (Figure 5, inset) and also by inserting the kinetic parameters obtained from the primary plot into the rate equation (*22*). There was excellent agreement between the two methods. $K_m^{\text{myristoyl-ACP}}$ was 1.6 ± 0.4 μM, and K_m^{proHlyA} was 3.6 ± 1.2 μM; V_{max} was 4667 ± 597 pmol of acyl group transferred min^{-1} mg^{-1}.

Use of an alternative substrate in the first half-reaction of a ping pong mechanism affects only the rate constants in the first half of the reaction, and various acyl-ACPs serve as acyl donors in the HlyC-catalyzed reaction (*10*). With all else being unchanged, at constant nonsaturating concentrations of either myristoyl-ACP or another acyl-ACP, double-reciprocal plots will show identical slopes for both substrates providing the kinetic mechanism is ping pong (*29*, *30*). Experiments were done like those described above, except that lauroyl-ACP was the acyl-group donor instead of myristoyl-ACP. Reaction rate measurements with respect to proHlyA at different fixed concentrations of lauroyl-ACP yielded parallel lines on a double-reciprocal plot of the same slope as those seen with myristoyl-ACP; these are shown as dotted lines in Figure 5. The best confirmation of parallel lines in double-reciprocal plotting is the half-reciprocal plot, S/v versus S, which requires convergence of all plots on the S/v axis (*29*). The data for both acyl-ACPs so plotted (not shown) gave common intercepts on half-reciprocal plots at different fixed concentrations of myristoyl-ACP and lauroyl-ACP, corroborating identical slopes on double-reciprocal plots and a ping pong mechanism for HlyC catalysis.

Table 2: Acyltransferase Activities of HlyC Single-Site Mutants[a]

	% of wild-type acyltransferase activity	
mutant	quick dilution	slowly refolded
S20A	ND[b]	50 ± 3
S19AS20A	ND	49 ± 1
S20C	ND	20 ± 0.4
S20T	ND	35 ± 2
S20H	ND	0
H23D	0	0
H23K	0	0
H23Y	11 ± 1	16 ± 2
Q43A	48 ± 7	77 ± 0.8

[a] Acyltransferase activity was measured as previously described (*10*) except that serine mutants were assayed with 2 μM fragment A instead of proHlyA. Quick dilution and slow refolding renaturation of HlyC were done as previously described (*13*). Slowly refolded wild-type His_6-S-tag-HlyC activity was 2.8 ± 0.09 nmol of acyl group transferred min^{-1} (mg of enzyme)$^{-1}$. Quickly diluted wild-type His_6-S-tag-HlyC activity was 1.9 ± 0.10 nmol of acyl group transferred min^{-1} (mg of enzyme)$^{-1}$. Data are the averages of at least three determinations of enzyme activity $\pm$ the standard deviation. Activities less than 5% of wild-type were interpreted as 0 activity. [b] ND: not determined. Quick dilutions of Ser20 mutations were not done since previous mutation of Ser20 showed no difference in activity between quick dilution and slow refolding (*13*).

Roles of Specific Residues. The roles of essential residue His23 and crucial residue Ser20 and another conserved residue of HlyC, Gln43, were investigated by site-directed mutation analysis (Table 2). The double mutation S19AS20A was made to assess the unlikely possibility that Ser19, a nonconserved residue, substituted partially for the critical function of conserved wild-type Ser20 in the mutant S20A (*13*). The double mutation had about the same activity as S20A; mutation of nonconserved Ser19 had no effect. Alteration of Ser20 to threonine, cysteine, or histidine residues increasingly impaired activity. The serine mutants with measurable activity were catalytically impaired in the same respect as previously reported Ser20 mutants (*13*), a diminished V_{max} and unchanged K_m (data not shown). Substitution of His23 by a tyrosine residue generated an enzyme that showed minimal activity in contrast to other previously reported mutations at this site, H23A, H23C, and H23S, which are inactive (*11*, *13*), and H23D and H23K (Table 2), which had no detectable activity. The method of refolding of H23Y did not influence activity. Mutation of Gln43 to alanine impaired activity to about half of wild-type upon quick dilution renaturation; if it was slowly

Table 3: Kinetic Parameters of Selected HlyC Mutants for Myristoyl-ACP and Different Internal Protein Acylation Substrates[a]

mutation	acyl-ACP K_m^{app}	acyl-ACP V_{max}^{app}	proHlyA K_m^{app}	proHlyA V_{max}^{app}	fragment A K_m^{app}	fragment A V_{max}^{app}
none	0.51 ± 0.2	2850 ± 324	2.0 ± 0.08	3060 ± 64	0.26 ± 0.05	2870 ± 179
H23Y	2.3 ± 0.3	691 ± 46	1.6 ± 0.09	293 ± 18	0.23 ± 0.09	317 ± 30
Q43A	0.48 ± 0.07	2130 ± 72	0.45 ± 0.08	1220 ± 53	0.058 ± 0.005	1830 ± 26

[a] For the determination of kinetic parameters at varying concentrations of myristoyl-ACP, [proHlyA] was 2 μM. When proHlyA or fragment A concentrations were varied, [myristoyl-ACP] was 1 μM. V_{max}^{app} values are pmol of myristate transferred min^{-1} (mg of enzyme)$^{-1}$. K_m^{app} and V_{max}^{app} are to 2 and 3 significant numbers, respectively, $\pm$ the standard deviation. Experimental details and procedures for calculating the kinetic constants and error estimates are given under Experimental Procedures.

refolded, however, activity increased to about three-fourths of wild-type.

The kinetic parameters of H23Y and Q43A are compared to wild-type in Table 3, and the efficacies of the interchangeable substrates proHlyA and fragment A are also contrasted. The V_{max} values for the two substrates were close; the increased substrate efficacy of fragment A shown above stemmed from its reduced K_m^{app} compared to proHlyA's K_m^{app}. Among five mutations of His23, only the tyrosine substitution supported detectable activity, although it was severely impaired at ~16% of the wild-type estimated reaction rate constant. The reduced catalytic efficiency of H23Y stemmed from an almost 5-fold higher myristoyl-ACP K_m^{app} and a reduced V_{max}^{app} compared to wild-type HlyC; the K_m^{app} values for proHlyA and fragment A were unaffected. In contrast, the K_m^{app} for either proHlyA or fragment A for the reaction catalyzed by mutant Q43A was actually reduced about 4-fold while that for myristoyl-ACP was unchanged compared to wild-type. The decreased catalytic efficiency of Q43A reported above stemmed from a reduced V_{max}^{app} compared to wild-type HlyC.

As previously shown, acyl-enzyme formation during catalysis is preceded by formation of a noncovalent binary complex of acyl-ACP and HlyC (~43 kDa) which is readily captured upon treatment with dimethyl suberimidate (*10*, *11*). All the serine mutants reported herein, the double mutation S19AS20A, S20T, S20H, S20C, and His23 mutations H23K and H23Y formed chemically cross-linked heterodimers comparable to wild-type (Figure 6). Acyl-HlyC formation by these same serine and histidine mutants was, however, greatly diminished or virtually undetectable with one exception; the inactive mutant H23K formed reduced but unequivocally detectable acyl-enzyme intermediate, the only inactive His23 mutant to do so (*11*, *13*). Q43A HlyC showed reduced heterodimer and reduced acyl-enzyme intermediate compared to wild-type.

The pH stability of the unproductive acyl-enzyme of H23K resembled but was not identical to the stability of wild-type acyl-enzyme even though less acyl-H23K was formed than acyl-HlyC from identical amounts of myristoyl-ACP and the respective enzymes (Figure 7). Owing to the differences in the amount of acyl-enzyme formed by wild-type and H23K HlyCs and analyzed simultaneously under identical conditions, the fluorogram illustrating acyl-HlyC was developed after 2 weeks of exposure, while that shown for acyl-H23K was developed at 4 weeks for optimum analysis (Figure 7). Acyl-H23K and acyl-wild-type HlyC tolerated basic conditions better than acidic and showed similar susceptibilities to hydroxylamine. Within this general pattern of similar attributes, there were differences which are expressed as the percent of the maximally stable form of each at pH 8.6. H23K at pH 6.5 had roughly 60% of its pH 8.6 stability; in contrast, wild-type at pH 6.5 was about 30% of the amount of wild-type at pH 8.6. There was a similar difference in response to hydroxylamine at pH 8.6 with H23K being more stable than wild-type, ~40% compared to 25%. Behavior consistent with amide linkages would match the gross similarities, and the slight differences would fit an acyl-histidine in wild-type and an acyl-lysine in H23K.

Wild-type HlyC and the mutant S20A, as a control, were treated with radiolabeled DFP, and there was no detectable label incorporation into either (data not shown). As previously reported, HlyC is not inhibited by serine-directed reagents (*13*). Although crucial for activity, Ser20 is not essential (*13*), and thus was unlikely to be the HlyC residue covalently modified during catalysis.

DISCUSSION

Fragment A was a more tractable and effective substrate for study of the acylation reaction compared to proHlyA. Comparison of kinetic parameters of proHlyA and fragment A measured under equivalent conditions indicated that the increased catalytic efficiency of fragment A stemmed from its decreased K_m, almost 10-fold less than that of proHlyA; the V_{max} of the reaction was about the same with either fragment A or proHlyA. This may imply that both substrates are acylated equally well after binding but fragment A more facilely binds to acyl-HlyC than does proHlyA. Alternatively, fragment A may function better because it is structurally more stable than proHlyA. This difference in behavior likely stems largely from the absence of the hydrophobic portion of proHlyA in fragment A (Figure 1), resulting in decreased aggregation. Use of the highly sensitive S-tag detection and anti-ACP antibodies, to investigate possible heterocomplex formation involving S-tagged fragment A during the forward reaction, showed no detectable ternary complex formation among fragment A, HlyC, and myristoyl-ACP. Lack of ternary complex formation corresponds with earlier findings regarding proHlyA, which does not complex with HlyC and myristoyl-ACP while the previously reported heterocomplex formation between myristoyl-ACP and HlyC upon treatment with dimethyl suberimidate was readily detected (*10*). These findings are in accord with the observed ping pong kinetic mechanism.

Previously reported evidence including demonstration of two independent partial reactions is summarized above. In addition, steady-state kinetics resulted in parallel lines on double-reciprocal plots for two acyl-donor substrates, myristoyl-ACP and lauroyl-ACP, asserting that the path of the second partial reaction proceeded independently of the first partial reaction, an affirmation of a ping pong mechanism (*30*, *31*, *34*). A sequential mechanism would describe plots intersecting on or to the left of the $1/v$ axis of a double-reciprocal plot rather than forming parallel lines.

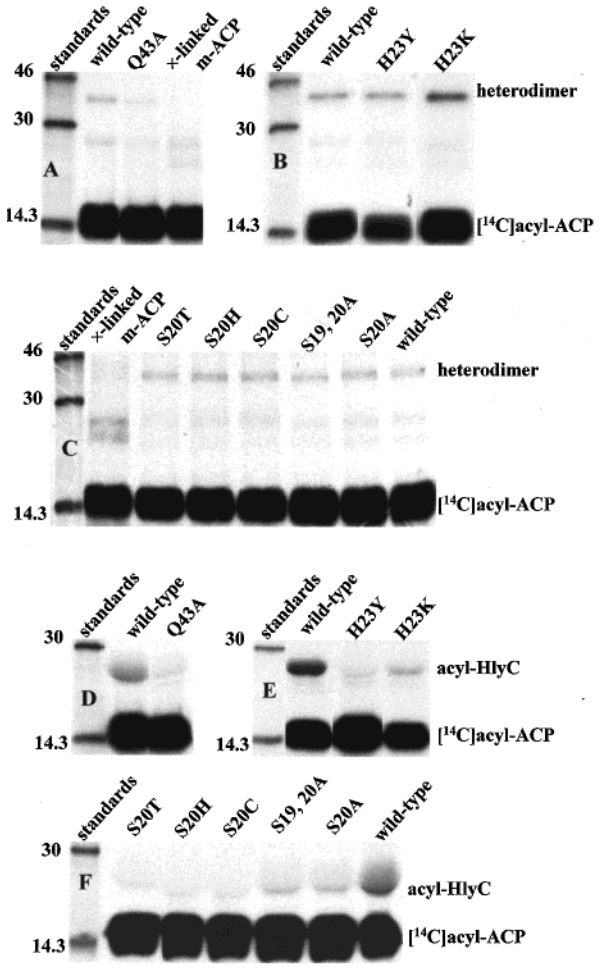

FIGURE 6: Binary complex and acyl-enzyme formations of HlyC wild-type and mutants with myristoyl-ACP. Mixtures of [^{14}C]-myristoyl-ACP and HlyC wild-type or mutants were prepared in the presence of dimethyl suberimidate (A−C) and without chemical cross-linking (D−F). Reactions in panels A−C contained 2 μM [^{14}C]myristoyl-ACP and 4.5 μM wild-type or mutant His_6-S-tag-HlyC and were assembled as described previously for assay of acyltransferase activity (*10*). Dimethyl suberimidate (10 mM) was added, and after 10 min at 25 °C, reaction was halted by adding 100 mM ammonium acetate. A reaction containing [^{14}C]myristoyl-ACP only was done as a reference. A reaction containing wild-type His_6-S-tag-HlyC was done with each set of mutant HlyC experiments to provide a reference for comparison. Reactions in panels D−F were assembled like those described above except that 3.8 μM [^{14}C]myristoyl-ACP and 50 μM wild-type or mutant His_6-S-tag-HlyC were added and incubated for 10 min 25 °C. No dimethyl suberimidate was added. Following incubation, proteins in all reactions were precipitated with 10% trichloroacetic acid at 4 °C, collected, dissolved in 20 μL of 2% SDS sample buffer that contained 4 M urea, and subjected to SDS−15% PAGE and fluorography as described under Experimental Procedures. Results depicted in panels A, B, D, E, and F were generated using the fluor Enhance, C Entensify. Radioactive mass standards were run, and kDa values are shown.

The hemolysin toxin acylation is the only protein internal acyltranferase that has been biochemically characterized (*9*−*11*, *13*, *34*), and this is, to our knowledge, the first description of a steady-state kinetic mechanism directly measuring transfer of fatty acyl groups to the internal residues of a protein. Analysis, performed in another laboratory, of the steady-state kinetic mechanism of hemolysin toxin activation by measuring erythrocyte lysis suggested a sequential kinetic mechanism (*35*), which is at variance with the extensive

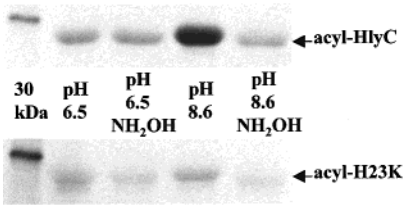

FIGURE 7: Acyl-H23K stability under different conditions compared to myristoyl-HlyC. [^{14}C]Acyl-HlyC, wild-type and H23K, formed under fixed conditions and subjected to different treatments from among those described in the Figure 4 legend as described under Experimental Procedures and then measured by SDS−15% PAGE separation, fluorography, and densitometric analysis. Film was developed for 2 weeks for analysis of wild-type acyl-HlyC and for 4 weeks for analysis of acyl-H23K.

evidence summarized above indicating a ping pong kinetic mechanism. The discrepancy likely stems from the measurement of different biochemical events, acyl transfer in contrast to lysis, where lysis is an occurrence of uncertain stoichiometry at least two steps removed from acyl transfer. The cytolytic action of the toxin activated in vitro consists of three separate biochemical events: (1) acylation of internal residues of the toxin; (2) binding of toxin to the target cell; and (3) lysis of the target cell following intra- and possibly intermolecular rearrangements of toxin (*36*−*40*). Separate biochemical study of each event is necessary for understanding what is transpiring at the molecular level in rendering a benign protein toxic and its subsequent lytic behavior.

The stabilities of the myristoyl-HlyC wild-type intermediate and myristoyl-HlyC C57A intermediate (a cysteine-less mutant) under various conditions validated previously reported (*13*) inhibitor and mutation studies indicating that the intermediate acyl-HlyC is neither a thio ester nor an oxygen ester. Reported speculation that the acyl-intermediate is actually a noncovalent ternary complex of acyl-ACP, HlyC, and proHlyA giving rise to a sequential kinetic mechanism (*35*) was ruled out because, among other facts, the stability of the ~23 kDa acyl-intermediate exhibited no resemblance to that of acyl-ACP, a thio ester. Moreover, a ternary complex would be considerably larger, ~142 kDa. An acid anhydride or ester bound acyl-enzyme intermediate would be expected to be least stable at pH 8.6 compared to pHs 8.0, 6.5, and 5.0; this was not the case for myristoyl-HlyC, which was most stable at pH 8.6. There are no conserved lysine residues among the hemolysin C protein (*11*); thus, an acyl-lysine, which would be more stable at pH 8.6 than at acidic pH, is not a likely intermediate. Myristoyl-HlyC became less stable as the pH decreased, a behavior like that reported for the intermediate formed by the active site histidine residue nucleophile in acid phosphatase (*41*). The increased stability of myristoyl-HlyC at basic pH compared to mild acidity is compatible with acylation of the imidazole ring N of a histidine residue. Although very reactive, such a structure would be more stable than an acid anhydride (*42*). As a structural approximation of such an intermediate, the hydrolysis of acyl-imidazole formed in nucleophilic catalysis by imidazole is the slow step of the overall reaction (*43*). Like acyl-imidazole, the myristoyl-HlyC intermediate was susceptible to breakdown by nucleophiles as illustrated by the effects of imidazole, hydroxylamine, and dithiothreitol. Furthermore, the reactive hydrolytic species is acyl-imidazolium and not free acyl-imidazole (*43*), which is compat-

ible with the increased stability of the acyl-enzyme observed at higher pH seen in Figures 4 and 7. His23 is the only conserved residue that could potentially bear an acyl group whose mutation results in total loss of activity (*11*). Furthermore, myristoyl-ACP protection from diethyl pyrocarbonate inhibition, a reagent specific for histidine residues, is consistent with His23 being in the active site proximity (*13*). The unique ability of H23K among His23 mutations to form acyl-HlyC while supporting no detectable acyl transfer to proHlyA or fragment A affirmed a special role for His23.

Histidine residues are crucial in many enzyme-catalyzed reactions as acid/base catalysts. A rare example of histidine functioning as a nucleophile in an acyl group transfer is the acyl-imidazole intermediate formed during enzymatic catalysis in the covalent binding of complement component C4 to the surface of pathogens (*44*). An internal thio ester of C4B is attacked intramolecularly by a histidine residue to form an acyl-imidazole intermediate, and the acyl group is subsequently transferred to amino or hydroxyl nucleophiles. This reaction is curiously analogous to proHlyA activation to HlyA, which entails proHlyA internal ϵ-amino group acylation by acyl transfer from the thio ester acyl-ACP via an acyl-HlyC, likely an acyl-imidazole, to the amino nucleophile. Notably, among several nucleophile-bearing residues substituted for the crucial histidine residue in C4B, only a mutant containing a tyrosine substituent was functional, albeit less effectively than the histidine containing wild-type (*45*). In HlyC, His23 also was replaceable with functional preservation only by tyrosine, and this was minimally functional compared to wild-type. The tyrosine phenolic group is a less effective nucleophile under the conditions employed than is the histidine imidazole nitrogen. In our view, when His23 was mutated to a lysine, the epsilon primary amino group of Lys23 was acylated, forming acyl-HlyC less than wild-type but more than H23Y (Figure 6). In contrast to the minimally active H23Y, H23K, although acylated, did not transfer its acyl group to proHlyA or fragment A. Nucleophilic attack by the primary amine of H23K formed an amide bond like that of the HlyC reaction product, which would not be a reactive acyl donor in contrast to acyl-histidine formed by wild-type. Acyl-H23K showed a pattern of pH stability consistent with an amide-bonded intermediate as did wild-type, but it was more stable than acyl-HlyC wild-type, presumably an acyl-imidazole. Acyl-imidazole with a free energy of hydrolysis greater than −13 000 cal/mol at pH 7, is thermodynamically unstable compared with most amides, esters, and thiol esters, and is highly susceptible to nucleophilic attack (*43*). In contrast to the proposed *N*-acyl-histidine of the wild-type, the acyl-enzyme of H23K, *N*-acyl-lysine, would not be expected to function in acyl group transfer. The fact that such transfer was not observed even though acyl-H23K was formed suggests that His23 is the site of acylation of HlyC.

ACKNOWLEDGMENT

We thank Dr. Gaston Schmir and Dr. Christina Zioudrou for helpful and inspiring discussions.

REFERENCES

1. Vassilev, A. A., Plesofsky-Vig, N., and Brambl, R. (1995) *Proc. Natl. Acad. Sci. U.S.A. 92*, 8680−8684.
2. Stevenson, F. T., Bursten, S. L., Fanton, C., Locksley, R. M., and Lovett, D. (1993) *Proc. Natl. Acad. Sci. U.S.A. 90*, 7245−7249.
3. Hedo, J. A., Collier, E., and Watkinson, A. (1987) *J. Biol. Chem. 262*, 954−957.
4. Olson, E. N., Glaser, L., and Merlie, J. P. (1984) *J. Biol. Chem. 259*, 5364−5367.
5. Towler, D., and Glaser, L. (1986) *Biochemistry 25*, 878−884.
6. Menestrina, G., Moser, C., Pellet, and Welch, R. (1994) *Toxicology 87*, 249−267.
7. Coote, J. G. (1992) *FEMS Microbiol. Rev. 88*, 137−162.
8. Nicaud, J.-M., Mackman, N., Gray, L., and Holland, I. B. (1985) *FEBS Lett. 187*, 339−344.
9. Stanley, P., Packman, L. C., Koronakis, V., and Hughes, C. (1994) *Science 266*, 1992−1996.
10. Trent, M. S., Worsham, L., and Ernst-Fonberg, M. L. (1998) *Biochemistry 37*, 4644−4652.
11. Trent, M. S., Worsham, L., and Ernst-Fonberg, M. L. (1999) *Biochemistry 38*, 9541−9548.
12. Guzmán-Verri, C., García, and Arvidson, S. (1997) *J. Bacteriol. 179*, 5959−5962.
13. Trent, M. S., Worsham, L., and Ernst-Fonberg, M. L. (1999) *Biochemistry 38*, 3433−3439.
14. Trent, M. S., Worsham, L., and Ernst-Fonberg, M. L. (1999) *Biochemistry 38*, 8831−8838.
15. Hess, J., Wels, W., Vogel, M., and Goebel, W. (1986) *FEMS Microbiol. Lett. 34*, 1−11.
16. Sanger, F., Nicklen, S., and Coulson, A. R. (1977) *Proc. Natl. Acad. Sci. U.S.A. 74*, 5463−5467.
17. Worsham, L. M., Williams, S., and Ernst-Fonberg, M. L. (1993) *Biochim. Biophys. Acta 1170*, 62−71.
18. Vuillard, L., Rabilloud, T., and Goldberg, M. E. (1998) *Eur. J. Biochem. 256*, 128−135.
19. Hattori, M., Adachi, H., Aoki, J., Tsujimoto, M., Arai, H., and Inoue, K. (1995) *J. Biol. Chem. 270*, 31345−31352.
20. Bradford, M. M. (1976) *Anal. Biochem. 72*, 748−754.
21. Laemmli, U. K. (1970) *Nature 227*, 680−685.
22. Wilkinson, G. N. (1961) *Biochem. J. 80*, 324−332.
23. Walker, T. A., Jonak, Z. L., Worsham, L. M. S., and Ernst-Fonberg, M. L. (1981) *Biochem. J. 199*, 383−392.
24. Trent, M. S. (1998) Ph.D. Dissertation, East Tennessee State University, Johnson City, TN.
25. Stanley, P., Koronakis, Hardie, and Hughes, C. (1996) *Mol. Microbiol. 20*, 813−822.
26. Felmlee, T., and Welch, R. A. (1988) *Proc. Natl. Acad. Sci. U.S.A. 85*, 5269−5273.
27. Ludwig, A., Jarchau, T., Benz, R., and Goebel, W. (1988) *Mol. Gen. Genet. 214*, 553−561.
28. Boehm, D. F., Welch, R. A., and Snyder, I. S. (1990) *Infect. Immun. 58*, 1959−1964.
29. Fromm, H. J. (1975) *Initial Rate Enzyme Kinetics*, pp 72−73, Springer-Verlag, New York.
30. Purich, D. L. (1982) *Methods Enzymol. 87*, 10−11.
31. Cornish-Bowden, A., and Wharton, C. W. (1988) *Enzyme Kinetics*, pp 30−31, IRL Press, Oxford, United Kingdom.
32. Purich, D., Ed. (1983) in *Contemporary Enzyme Kinetics and Mechanism*, p 354, Academic Press, New York.
33. Rudolph, F. B., and Fromm, H. J. (1988) in *Contemporary Enzyme Kinetics and Mechanism* (Purich, D. L., Ed.) pp 60−61, Academic Press, New York.
34. Issartel, J.-P., Koronakis, V., and Hughes, C. (1991) *Nature 351*, 759−761.
35. Stanley, P., Hyland, C., Koronakis, V., and Hughes, C. (1999) *Mol. Microbiol. 34*, 887−901.
36. Moayeri, M., and Welch, R. A. (1997) *Infect. Immun. 65*, 2233−2239.
37. Bauer, M. E., and Welch, R. A. (1996) *Infect. Immun. 64*, 167−175.
38. Pellett, S., and Welch, R. A. (1996) *Infect. Immun. 64*, 3081−3087.
39. Ludwig, R., Benz, R., and Goebel, W. (1993) *Mol. Gen. Genet. 241*, 89−96.

40. Ludwig, A., Garcia, R., Bauer, S., Jarchau, T., Benz, R., Hoppe, J., and Goebel, W. (1996) *J. Bacteriol. 178*, 5422−5430.
41. McTigue, J. J., and Van Etten, R. L. (1978) *Biochim. Biophys. Acta 523*, 407−421.
42. Bender, M. L., Bergeron, R. J., and Komiyama, M. (1984) *The Bioorganic Chemistry of Enzymatic Catalysis*, pp 140−152, John Wiley & Sons, New York.
43. Jencks, W. P. (1969) *Catalysis in Chemistry and Enzymology*, pp 67−71, McGraw-Hill, New York.
44. Dodd, A. W., Ren, X., Willis, A., and Law, S. K. A. (1996) *Nature 379*, 177−179.
45. Ren, X., Dodds, A. W., Enghild, J. J., Chu, C. T., and Law, S. K. A. (1995) *FEBS Lett. 368*, 87−91.

BI011032H